Low-temperature dielectric properties and phase transition in $BaMnF_4$†

G. A. Samara and Peter M. Richards
Sandia Laboratories, Albuquerque, New Mexico 87115
(Received 7 June 1976)

The temperature dependences of the static dielectric properties of $BaMnF_4$ were investigated from 4 to 300 K at 1 kHz to 9.8 GHz with emphasis on the behavior near the structural phase transition at 247 K. Anomalies in the dielectric constants ϵ'_i and losses $\tan\delta_i$ at the transition were observed along the major crystallographic directions, the main feature being a λ-shaped anomaly in ϵ' along the polar a axis. This anomaly persists to very high frequencies (9.8 GHz). Anomalies were also observed in ϵ'_a at ~ 30 K and in ϵ'_b at ~ 70 K. These are believed to be related to the onset of spin ordering at these two temperatures. The effects of pressure on the dielectric properties and transition temperature T_c were also investigated. T_c increases nonlinearly with pressure at low pressures, reaches a maximum and then decreases at higher pressures. This is discussed briefly in terms of the lattice-dynamical origin of the transition. The crystal is highly anisotropic and this is reflected in the ϵ'_i. This anisotropy is due to the lattice contribution to ϵ'_i and specifically the relevant lattice resonance frequencies. The over-all results and their implications are discussed.

I. INTRODUCTION

$BaMnF_4$ is an important member of a group of isomorphous crystals of the $BaM^{2+}F_4$ type (M = Mg, Zn, Mn, Fe, Co, and Ni). At ambient conditions these crystals are orthorhombic (space group C_{2v}^{12}-$A2_1am$), the structure consisting of layered sheets of linked MF_6 octahedra with the layer planes normal to the b axis and with the Ba ions located between the layers.[1] The crystals are strongly piezoelectric and pyroelectric—some exhibit reversal of the spontaneous polarization at electric fields below the breakdown strength and can thus be classified as ferroelectrics.[2,3] In $BaMnF_4$ the polarization cannot apparently be reversed presumably due to unfavorable Mn-F and Mn-Mn interionic distances[1] as well as to the relatively high electrical conductivity of this crystal ($\sigma_a \simeq 1\times10^{-6}\ \Omega^{-1}\,\mathrm{cm}^{-1}$).[3] Several of the crystals also become antiferromagnetically ordered at low temperatures (Neél temperature $T_N \simeq 26$ K for $BaMnF_4$).[4]

The temperature dependences of the static dielectric constants of these crystals have been reported for $T > 300$ °K.[5] It is found that the strain-free (clamped) dielectric constant along the two-fold pyroelectric a axis obeys a Curie-Weiss law at temperatures near the melting point. An interesting feature is that in all cases the extrapolated Curie-Weiss temperature is found to be higher than the melting point.

One important feature which distinguishes $BaMnF_4$ from its isomorphs is the existence in this crystal of a second-order structural phase transition at ~250 °K. The transition was first observed in ultrasonic-attenuation measurements by Spencer *et al.*[6] and was later studied by Ryan and Scott[7] using Raman scattering and by Fritz using ultrasonic velocity[8] and attenuation[9] techniques. The Raman results indicated that the transition is associated with the softening of an optical phonon at the zone boundary of the high-temperature orthorhombic (C_{2v}^{12}) phase and involves doubling of the primitive unit cell below T_c. However, the symmetry (eigenvector) of the soft mode above T_c and the crystal structure below T_c have not been determined. Furthermore, an inelastic-neutron-scattering study[10] indicates that the transition is more complicated than suggested by the Raman results and involves more than a simple doubling of the unit cell.

In the absence of detailed knowledge of the properties of the transition as well as of the phonon spectra above and below T_c, it is of interest to study the properties of $BaMnF_4$ near T_c and to seek evidence for any coupling of the soft mode to other excitations in the crystal. Toward this end we have investigated the temperature dependence of the static dielectric properties of $BaMnF_4$ with emphasis on the behavior near T_c. The static dielectric constants ϵ_i relate to the long wavelength ($\vec{q}=0$) infrared-active optic phonons of the crystal. Anomalies in these constants at T_c are found along the three crystallographic axes. We have also investigated the effects of hydrostatic pressure on the ϵ_i near T_c and thereby determined the pressure dependence of T_c. A further interesting feature is that two- and three-dimensional spin ordering occur in $BaMnF_4$ at low temperatures. To seek possible evidence for the manifestation of this ordering in the $\epsilon_i(T)$ response, the measurements were ex-

tended down to 4 K. Anomalies were observed along the a and b axes. In what follows, we shall present the results and their interpretation.

II. EXPERIMENTAL DETAILS

Measurements were made on single-crystal samples cut in the form of thin plates 0.5–1.4 mm thick and 0.20–0.38 cm^2 in area and oriented with the thickness dimension along one of the orthorhombic (C_{2v}^{12}) a, b, or c axes. Electrodes were vapor deposited on the large sample faces and consisted of a thin layer of chromium followed by a thin layer of gold. Detailed capacitance and dielectric-loss measurements were made in the 1–100-kHz frequency range employing transformer ratio arm bridges (General Radio model 1615A) or Hewlett-Packard model 4270A) equipped with three terminal connections. Shielded leads and sample holders were used. The measurements along the a axis were extended to higher frequencies. Data to 70 MHz were obtained using a Wayne Kerr bridge (model B 801), and an experiment was performed at 9.8 GHz using microwave techniques. In this latter case a cube shaped sample was placed inside a microwave cavity with the a axis parallel to the rf electric field and the dielectric constant was deduced from the shift of the resonance frequency of the cavity.

The temperature (4–350 K) and pressure (0–8 kbar ≡ 0.8 GPa) measurements were made in a maraging steel pressure cell mounted in a conventional low-temperature Dewar. The procedures were similar to those described earlier.[11] Helium gas was the pressure fluid, and the pressure was measured to better than 1% by a calibrated Manganin gauge. Temperature changes were measured to ±0.10 K using CU-constantan and Cu-AuFe thermocouples.

In the absence of thermal-expansion and compressibility data on $BaMnF_4$, the real (ϵ') and imaginary (ϵ'') parts of the dielectric constant and their changes with temperature and pressure were calculated directly from the measured sample capacitance and loss without correcting for changes in sample dimensions owing to expansion and compression. However, such corrections are usually small and do not affect the main conclusions of this work.

III. RESULTS AND DISCUSSION

A. Magnitude of the dielectric constants

$BaMnF_4$ is a highly anisotropic crystal and this is reflected in the dielectric constants. At 290 K and 1 bar the values of the real parts of these constants are $\epsilon_a' = 12.4$, $\epsilon_b' = 20.9$, and $\epsilon_c' = 8.6$. The absolute accuracy of these values is limited to only ~±7% mainly owing to uncertainties in sample dimensions caused by the relatively small and irregular crystals available. The magnitude and anisotropy of the ϵ_i' deserve some comment. For an ionic crystal ϵ' is given by

$$\epsilon' = \epsilon_\infty' + \epsilon_l' , \tag{1}$$

where ϵ_∞' is the high-frequency or optical dielectric constant ($\equiv n^2$, where n is the appropriate refractive index in the limit of long wavelengths) and ϵ_l' is the lattice contribution. ϵ_∞' is determined solely by the electronic polarizabilities of the ions in the crystal, whereas ϵ_l' is determined by the lattice polarizabilities associated with the opposite displacements of the positive and negative ions in the course of long-wavelength transverse-optic vibrations and is of the form[12]

$$\epsilon_l' = \frac{4\pi(Ze^*)^2}{\mu v \omega_t^2}\left(\frac{\epsilon_\infty' + 2}{3}\right)^2 \equiv A\left(\frac{\epsilon_\infty' + 2}{3}\right)^2 . \tag{2}$$

Here Z is the valence, e^* is the Szigeti effective ionic charge, μ is the reduced mass of the ions, v is the volume per molecule, and ω_t is the appropriate lattice resonance frequency. The electronic polarizabilities of the ions influence ϵ_l' in two different ways: first via the effective ionic charge e^*—a short-range effect—and secondly, via the electronic enhancement factor $[\frac{1}{3}(\epsilon_\infty + 2)]^2$ which arises from long-range interactions between electronic and ionic displacements.

The room-temperature values of n_i for $BaMnF_4$ are[13] $n_a = 1.499$, $n_b = 1.48$, and $n_c = 1.505$ yielding $\epsilon_{\infty,a}' = 2.25$, $\epsilon_{\infty,b}' = 2.19$, and $\epsilon_{\infty,c}' = 2.26$. The values of $\epsilon_{l,i}'$ at 290 K are then $\epsilon_{l,a}' = 10.2$, $\epsilon_{l,b}' = 18.7$ and $\epsilon_{l,c}' = 6.3$. From these values it is clear that the large anisotropy in the ϵ_i' is associated with the lattice polarizabilities, and in particular the term A in Eq. (2). Some of this anisotropy may be due to anisotropy in the e_i^*, but it is more likely due to that in the $\omega_{t,i}$. Furthermore, since $e^* \leq e$, the electronic charge, it can be concluded that the relatively large $\epsilon_{l,b}'$ must be largely associated with a low value of $\omega_{t,b}$. Unfortunately, the ir resonance frequencies of $BaMnF_4$ apparently have not been measured at room temperature in order to allow us to check these conclusions quantitatively. Raman measurements have been made in the low-temperature phase and show that at $T \ll T_c$ the lowest phonons with a-, b-, and c-axis (orientations based on the high-temperature structure) polarizations lie at ~40, 28, and 105 cm^{-1}, respectively.[7] If the symmetry of the low-temperature phase is indeed $P2_1$,[9] or something of comparably low symmetry, then these modes will be ir active also. Since the anisotropy in the ϵ_i' in the low-temperature phase is (as will be seen later)

comparable to that in the high-temperature phase, it appears that the anisotropy in the phonon frequencies is qualitatively in the manner needed to account for the anisotropy in $\epsilon'_{i,i}$.

B. Temperature dependence of the dielectric constants

The temperature dependence of ϵ' along the pyroelectric a axis at 100 KHz is shown in Fig. 1. It is seen that ϵ'_a exhibited a λ-shaped anomaly at the 250-K transition. The low-temperature asymmetry of the $\epsilon'_a(T)$ anomaly can be understood as follows. Above T_c there is of course no linear coupling of the soft mode (a short-wavelength mode) to any zone center ($\vec{q}=0$) ir-active mode. Below T_c, on the other hand, the soft mode couples to the polarization and the more gradual decrease in ϵ'_a with decreasing T reflects the gradual buildup of the order parameter of the second-order transition as T moves away from T_c.

The $\epsilon'_a(T)$ response in Fig. 1 is frequency independent at frequencies $>\sim 100$ kHz, but strong frequency dependence is observed at lower frequencies and temperature $>\sim 220$ K. This is shown in Fig. 2. In the temperature regime of Fig. 2 the dielectric loss $\tan\delta$ is also strongly frequency dependent below 100 KHz and increases very rapidly with increasing T. This is shown in Fig. 2 expressed as $\epsilon''_a(T)$, where $\epsilon''_a = \epsilon'_a \tan\delta$. These large increases in ϵ'_a and ϵ''_a with increasing T at low frequencies are associated with the large increase in the conductivity of the crystal.[14] In Fig. 2 we note that there is a small anomaly in $\epsilon''_a(T)$ at the transition at 100 kHz. At 10 and 1 kHz the dielectric losses are so high that the anomaly is washed out on the logarithmic scale used, and only a change in the slope of the $\epsilon''_a(T)$ response is seen at T_c. Finally, we note that in Fig. 2 there is indicated some frequency dependence in $\epsilon'_a(T)$ above and below T_c at 30 MHz—specifically the $\epsilon'_a(T)$ curve at 30 MHz falls above that at 100 kHz. This is probably not a real effect, since accurate measurements in this MHz range are difficult, and we point out that ϵ'_a at 30 MHz was arbitrarily normalized at T_c to its value at 100 kHz.

At $T \ll T_c$, ϵ'_a decreases slowly with decreasing T in a manner typical of normal ionic dielectrics. This decrease continues until ~30 K, at which temperature another $\epsilon'_a(T)$ anomaly sets in (see inset in Fig. 1). This anomaly represents an additional decrease in ϵ'_a with decreasing T over that due to lattice effects. The cause of this anomaly is discussed briefly in Sec. III D.

Figure 1 also shows the $\epsilon'_c(T)$ response of $BaMnF_4$ at 100 kHz. In this case a small anomaly is observed at T_c below which the response is normal, ϵ'_c decreasing slowly with decreasing T and $d\epsilon'_c/dT \to 0$ as $T \to 0$ K. Above T_c, ϵ'_c and ϵ''_c exhibit qualitatively the same frequency and temperature dependences of ϵ'_a and ϵ''_a, except that ϵ''_c is a factor of ~20–30 lower than ϵ''_a.

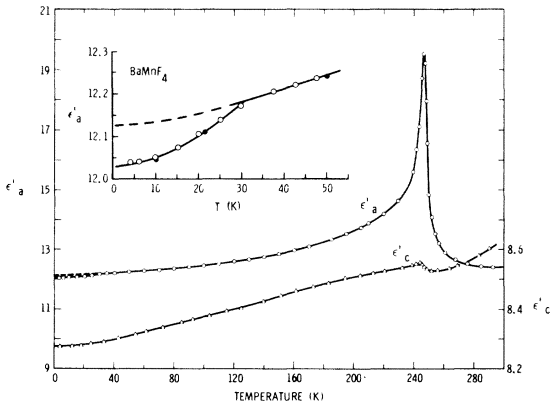

FIG. 1. Temperature dependences of the real parts of the a- and c-axis static dielectric constants of $BaMnF_4$ measured at 100 kHz and 1 bar. The inset shows the behavior of ϵ'_a at low temperatures, where the open and solid circles represent data taken on decreasing and increasing temperature, respectively.

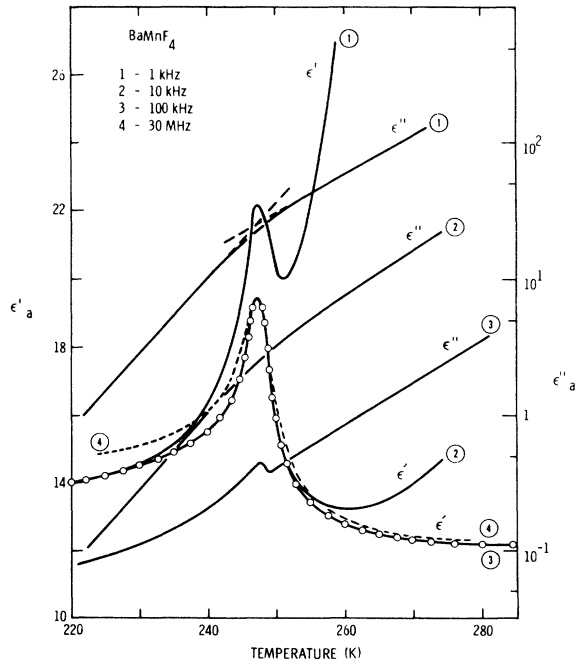

FIG. 2. Temperature dependences of the real and imaginary parts of the a-axis static dielectric constant of $BaMnF_4$ in the vicinity of the phase transition measured at different frequencies. For clarity actual data points are shown only for $\epsilon'_a(T)$ at 100 kHz.

The temperature dependence of ϵ_b' is shown in Fig. 3. This response is quite different than those along the a and c axes. ϵ_b' increases with decreasing T on both sides of the transition with only a change in slope at or near T_c. In the absence of detailed knowledge about the temperature dependence of the ir-active phonon frequencies and the lattice strain accompanying the transition, it is not possible to explain the shape of the $\epsilon_b'(T)$ response around T_c. An especially noteworthy feature in Fig. 3 is the relatively large decrease in ϵ_b' below ~70 K. The cause of this effect is discussed briefly in Sec. III D. Above ~250 K the frequency and temperature effects shown are a result of the high conductivity of the crystal. The inset in the figure shows $\epsilon''(T)$ near T_c at 100 kHz. At 10 and 1 kHz ϵ_b'' is much larger and the anomaly at T_c is washed out.

C. Nature of the transition and pressure dependence of T_c

As indicated in Sec. I, the Raman studies of Ryan and Scott[7] indicated that the phase transition at ~250 K is associated with a zone-boundary soft optical phonon. This conclusion was based on measurements below T_c which showed a soft optic mode whose frequency vanished at T_c with no evidence for the mode above T_c. Since all optic modes of the high-temperature phase's C_{2v} point group are Raman active, it was concluded that the soft mode below T_c corresponds to a zone-boundary phonon of the high-temperature phase, and thus the transition involves doubling of the primitive unit cell below T_c. On this basis it has been suggested[9,15] that the low-temperature structure should be monoclinic (space group $P2_1$), but this remains unconfirmed. Single-crystal x-ray-diffraction studies[16] show no definite evidence for the transition, thus emphasizing its subtle nature. A mechanism for the transition, based on the known Raman, ultrasonic, and other data, has been proposed.[9] It involves rotations of the MnF_6 octahedra about the orthorhombic b axis, with a pair of phonons at the Brillouin-zone S points $\pi\,(0, 1/b, \pm 1/c)$ being the soft modes. Though consistent with the then available data, this mechanism is not strictly correct. Inelastic-neutron-scattering work at Brookhaven[10] indicates that the soft mode is more complicated than was suggested by the Raman work. Specifically, the neutron results suggest that the wavelength of the soft mode is incommensurate with the lattice. At any rate, however, it is certain that the transition involves a short-wavelength soft optic phonon which most likely involves the rotations of adjacent MnF_6 octahedra. In this latter regard the $BaMnF_4$ transition is qualitatively similar to the well-known soft-mode transitions in $SrTiO_3$ and $Gd_2(MoO_4)_3$. However, from the standpoint of the dielectric response the $BaMnF_4$ transition is different in important respects. In $SrTiO_3$ the structural phase transition is strictly antiferrodistortive, the soft mode being nonpolar and there are no dielectric constant anomalies. In $Gd_2(MoO_4)_3$ there is a dielectric-constant anomaly along the c axis at T_c (qualitatively similar to the ϵ_a' anomaly in Fig. 1), but this anomaly is strain induced, being simply a manifestation of piezoelectric coupling.[17,18] It disappears when the crystal is clamped, i.e., for measurements at frequencies above the mechanical resonance frequency of the crystal. In $BaMnF_4$ the ϵ_a' anomaly persists in the clamped case. As shown in Fig. 4, the anomaly is still present at 9.8 GHz, i.e., well above any mechanical resonances. Thus, on the basis of this evidence and the asymmetry in the $\epsilon_a'(T)$ response in Fig. 1, it is evident that in the low-temperature phase of $BaMnF_4$ the soft mode couples linearly to the polarization with the coupling constant going to zero at T_c, whereas in the high-temperature phase there is no linear coupling.

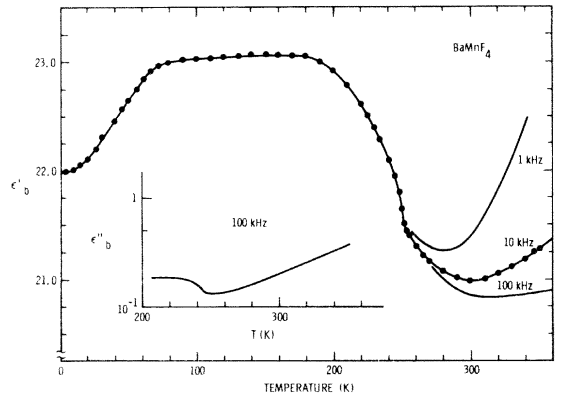

FIG. 3. Temperature dependence of the real part of the b-axis static dielectric constant of $BaMnF_4$ measured at different frequencies. Actual data points are shown only for the 10-kHz response. The inset shows the temperature dependence of the imaginary part of the dielectric constant at 100 kHz in the vicinity of the phase transition.

Previous work on $BaMnF_4$ has indicated that T_c varies among samples from different batches. Values from 249 to 255 K have been reported.[6-9] It has been suggested[19] that this variation in T_c may be due to the presence of small amounts of Mn^{3+} in $BaMnF_4$ crystals, the large size mismatch between Mn^{3+} and Mn^{2+} ions playing an important role. At present this remains a speculation which has not been confirmed. If in Fig. 1 we take the peak in the $\epsilon_a'(T)$ response as repre-

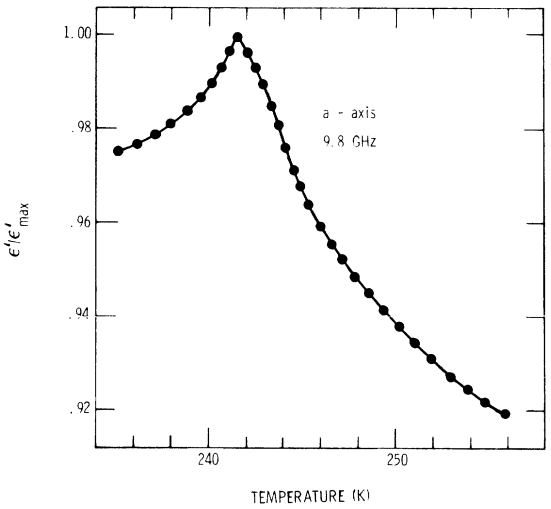

FIG. 4. Temperature dependence of the real part of the a-axis dielectric constant of $BaMnF_4$ at 9.8 GHz normalized to its peak value.

senting T_c, we get $T_c = 247.2 \pm 0.5$ K. This peak is a very well-defined feature and is easily reproducible. Along the b axis it is more difficult to determine T_c accurately. There is, however, in the $\epsilon_b'(T)$ response a distinct and reproducible change in slope in the region of T_c (see Fig. 3). It is felt that the peak in ϵ_a' is likely the most representative feature in the dielectric response of the true T_c of the crystal, and we take it as such. We should note, however, that ϵ_a' was observed to peak at a lower temperature at 9.8 GHz than at the lower frequencies. This behavior may be due in part to the fact that a different sample was used for the 9.8-GHz experiment.

The pressure dependence of T_c was measured by examining the effects of pressure on the $\epsilon_a'(T)$ and $\epsilon_b'(T)$ responses near T_c. Figure 5(a) shows typical $\epsilon_a'(T, P)$ results. In this as well as in the $\epsilon_b'(T, P)$ response the main effect of pressure is a simple displacement of the curves along the temperature axis towards higher temperatures. Another more subtle effect in Fig. 5(a) is a narrowing of the ϵ_a' anomaly (at T_c)—the narrowing is mostly on the low-temperature side and corresponds to a faster buildup of the order parameter at higher pressures.

Figure 5(b) shows the increase in the transition temperature with pressure deduced from the $\epsilon_a'(T, P)$ response. The initial slope is $dT_c/dP = 3.3$ K/kbar. The increase of T_c with hydrostatic pressure appears to be characteristic of displacive phase transitions associated with soft zone-boundary (or short-wavelength) optic phonons.[20] This is to be contrasted with the behavior of crystals which exhibit displacive transitions associated with soft zone-center polar optic phonons where T_c decreases with pressure. This difference in behavior has been interpreted in terms of a reversal in the roles of the short-range and long-range forces in the lattice dynamics of the two cases.[20] Specifically, for the zone-center soft modes the balance of forces leading to an imaginary harmonic mode frequency and soft-mode behavior is due to the overcancellation of the short-range forces by the negative Coulomb forces, whereas for the zone-boundary soft modes the overcancellation is by the short-range forces which are negative, i.e., attractive. Pressure affects this balance of forces differently in the two cases (the short-range forces being more strongly pressure dependent), and this provides a qualitative explanation for the observed pressure effects.[20]

An interesting feature of the results in Fig. 5(b) is the highly nonlinear $T_c(P)$ response over the relatively small pressure range covered. The nonlinearity appears to be more than could be accounted for on the basis of a reasonable de-

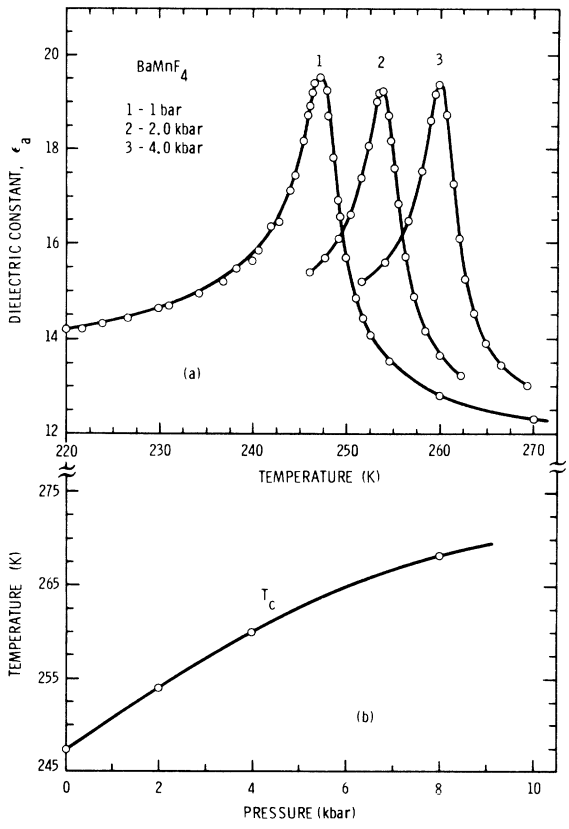

FIG. 5. (a) Effects of hydrostatic pressure on the $\epsilon_a'(T)$ response of $BaMnF_4$. (b) Shift of the structural-phase-transition temperature T_c with hydrostatic pressure.

crease in compressibility with pressure. Similar nonlinear $T_c(P)$ responses at relatively low pressures have been observed in other materials exhibiting soft short-wavelength optic phonons.[21] By comparison, $T_c(P)$ responses associated with soft zone-center optic modes tend to be relatively more linear over wider pressure ranges.[22] It is tempting to suggest that the highly nonlinear increases in the case of the short-wavelength soft phonons is to be expected, and, furthermore, that a reversal of the sign of dT_c/dP might be expected at sufficiently high pressure. This is because as we compress the ions closer and closer together the short-range interactions could not be expected to continue to be attractive. Ultimately, they must become repulsive.

In order to test this hypothesis the measurements of $\epsilon_a'(T,P)$ were extended to 18 kbar. To reach this pressure it was necessary to employ a different pressure apparatus than was used for the results presented thus far. A piston-cylinder apparatus using silver chloride as the pressure-transmitting medium was used. The $BaMnF_4$ sample was a small thin plate with leads attached to the large faces and was embedded in the silver chloride. The pressure generated in this apparatus is quasihydrostatic. The finite yield strength of the silver chloride causes some nonhydrostatic stresses. It is believed that these stresses are responsible for the broadening of $\epsilon_a'(T)$ anomaly at T_c that was observed in this experiment. Nevertheless, a well-defined $\epsilon_a'(T)$ peak was observed at all pressures. The shift of this peak (taken as representing T_c) with pressure is shown in Fig. 6. These results clearly show the postulated reversal in the sign of dT_c/dP.

It should be emphasized that the pressure effects in Fig. 6 were completely reversible with no evidence for any permanent effects of the nonhydrostatic stresses on the $\epsilon_a'(T,P)$ response. These nonhydrostatic stresses are, however, apparently responsible for the significantly lower initial (i.e., low pressure) value of dT_c/dP in Fig. 6 as compared with the hydrostatic pressure data in Fig. 5(b) (2.0 vs 3.3 K/bar).

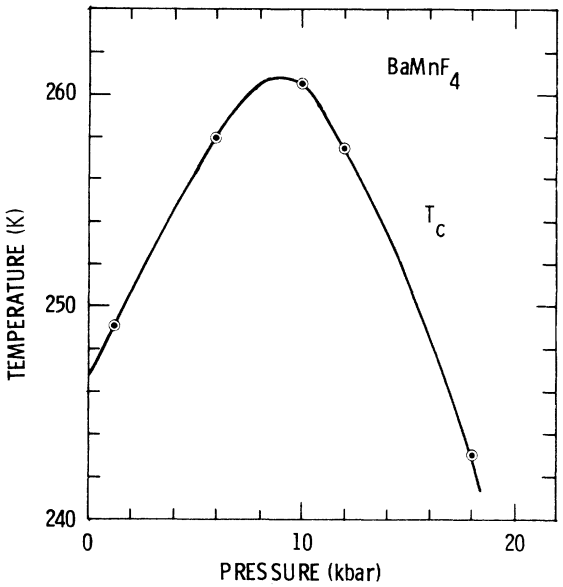

FIG. 6. Shift of the structural-phase-transition temperature T_c of $BaMnF_4$ with quasihydrostatic pressure.

D. Low-temperature anomalies and relationship to magnetic ordering

As we have pointed out earlier (see Figs. 1 and 3), dielectric-constant anomalies are observed in $BaMnF_4$ starting (on cooling) at ~30 K for ϵ_a' and at ~70 K for ϵ_b'. These anomalies represent decreases in ϵ_i' over and above the lattice contribution. No anomaly is seen in ϵ_c' in the comparable temperature range. The factors that make these anomalies of considerable interest are (i) the ϵ_a' anomaly occurs at the Neél temperature, (ii) the ϵ_b' anomaly occurs at or near the temperature where in-plane (i.e., two-dimensional) ordering of the Mn-ion spins along the b axis begins, and (iii) there are low-lying polar optic phonons with polarization along the a axis (at ~40 cm^{-1}) and the b axis (at ~28 cm^{-1}). Furthermore, the magnetic susceptibility is isotropic in the ac plane, but the lowest-lying polar phonon with c-axis polarization is at ~105 cm^{-1}, and there is no ϵ_c' anomaly at T_N. These observations have led to the conclusion[23] that the ϵ_a' and ϵ_b' anomalies must be related to the magnetic properties and in particular may result from coupling between long-wavelength polar optic phonons and ordered spins. While the possibility of such coupling has been raised,[24] we know of no prior experimental evidence for it. A more detailed description and explanation of the observed ϵ_i' anomalies will be presented elsewhere.[23]

ACKNOWLEDGMENTS

We express our thanks to B. E. Hammons for expert technical assistance and to Dr. E. L. Venturini, Dr. I. J. Fritz and Dr. P. S. Peercy for helpful discussions. The samples used were cut from crystals grown at MIT by Dr. A. Linz and Dr. D. Gabbe and kindly provided to us by Professor F. R. Morgenthaler. We are also especially thankful to Professor J. F. Scott for introducing us to the interesting properties of $BaMnF_4$.

†Work supported by U. S. Energy Research and Development Administration under Contract No. AT (29-1) 789.

[1]E. T. Keve, S. C. Abrahams, and J. L. Bernstein, J. Chem. Phys. 51, 4828 (1969).

[2]M. Eibschütz and H. J. Guggenheim, Solid State Commun. 6, 737 (1968).

[3]M. Eibschütz, H. J. Guggenheim, S. H. Wemple, I. Camlibel, and M. DiDomenico, Jr., Phys. Lett. A 29, 409 (1969).

[4]L. M. Holmes, M. Eibschütz, and H. J. Guggenheim, Solid State Commun. 7, 973 (1969); M. Eibschütz *et al.*, J. Appl. Phys. 41, 943 (1970); Phys. Rev. B 6, 2677 (1972).

[5]M. DiDomenico, M. Eibschütz, H. J. Guggenheim, and I. Camlibel, Solid State Commun. 7, 1119 (1969).

[6]E. G. Spencer, H. J. Guggenheim, and G. J. Kominiak, Appl. Phys. Lett. 17, 300 (1970).

[7]J. F. Ryan and J. F. Scott, Solid State Commun. 14, 5 (1974); in Proceedings of the Third International Conference on Light Scattering in Solids, edited by M. Balkanski *et al.* (Flammarion, Paris, to be published).

[8]I. J. Fritz, Phys. Lett. A 51, 219 (1975).

[9]I. J. Fritz, Phys. Rev. Lett. 35, 1511 (1975).

[10]S. M. Shapiro, R. A. Cowley, D. E. Cox, M. Eibschütz, and H. J. Guggenheim, Proceedings of Conference on Neutron Scattering, Gatlingburg, Tenn., 1976 (unpublished).

[11]G. A. Samara and P. S. Peercy, Phys. Rev. B 7, 1131 (1973).

[12]B. Szigeti, Trans. Faraday Soc. 45, 155 (1949).

[13]Data from Ref. 2. In this reference the refractive indices are given at only one wavelength (589.3 μm). It is assumed that the magnitude and anisotropy in these indices do not change appreciably with frequency.

[14]The conductivity results are to be published elsewhere.

[15]V. Dvorak, Phys. Status. Solidi B 71, 269 (1975).

[16]B. Morosin (private communication).

[17]L. E. Cross, A. Fouskova, and S. E. Cummins, Phys. Rev. 21, 812 (1968).

[18]J. D. Axe, B. Dorner, and G. Shirane, Phys. Rev. Lett. 26, 519 (1971).

[19]J. F. Scott, in Vibration Spectra and Structure, edited by J. R. Durig (Elsevier, Amsterdam, to be published).

[20]G. A. Samara, T. Sakudo, and K. Yoshimitsu, Phys. Rev. Lett. 35, 1767 (1975).

[21]G. A. Samara, Phys. Rev. B 1, 3777 (1970).

[22]G. A. Samara, Phys. Rev. 151, 378 (1966); Ferroelectrics 7, 221 (1974); 9, 209 (1975).

[23]G. A. Samara and J. F. Scott (unpublished).

[24]R. Englman and H. Wyatom, in *Magnetoelectric Interaction Phenomena in Crystals*, edited by A. J. Freeman and H. Schmid (Gordon and Breach, New York, 1975), p. 17.